Proceedings of the 2019 Winter Simulation Conference
N. Mustafee, K.-H.G. Bae, S. Lazarova-Molnar, M. Rabe, C. Szabo, P. Haas, and Y.-J. Son, eds.

VERIFICATION METHODOLOGY FOR DISCRETE EVENT SIMULATION MODELS OF PERSONNEL IN THE CANADIAN ARMED FORCES

Jillian Anne Henderson
Robert M. Bryce

Director General Military Personnel Research and Analysis
Department of National Defence
Ottawa, ON K2H 8E9, CANADA

ABSTRACT

The Canadian Armed Forces (CAF) uses a variety of tools to model, forecast and investigate workforce behavior; one such tool is a custom Discrete Event Simulation (DES) framework designed to address military Human Resources (HR) and personnel questions called the Force Flow Model (FFM). In this work we propose a methodology to verify workforce simulations and we discuss its use for verification of the FFM. We demonstrate precise agreement with an analytic model when the FFM parameters are matched to exactly solvable analytic scenarios. The methodology is simple to understand and apply, is generally applicable to workforce simulations, and helps to meet the need to verify simulations by providing known analytic results to benchmark against.

1 INTRODUCTION

In 2016, the Royal Canadian Navy (RCN) requested a tool that could model their personnel with the ability to vary parameters to conduct "what if" scenarios. A Discrete Event (DES) model was constructed that simulates a military member's journey through recruitment, occupational training, rank progression, and eventual release. This Force Flow Model (FFM) is to be applied to complex situations where there is no known ground truth. Here, we introduce a verification methodology that provides a strong verification test against exactly known results. In effect, the simulation is treated as a black box and we carefully select parameters that place the simulation into a scenario where analytically testable results can be obtained, providing an exact benchmark. By ensuring accurate performance under these verification parameters, we gain confidence the simulation will behave properly under other settings which will address the "what if" scenarios of interest to the Canadian Armed Forces (CAF).

Any model of a system that will be potentially used for decision making should undergo a transparent process of verification and validation. Verification will increase confidence that its implementation performs as expected under specialized testing and validation will show that the end product accurately represents its intended application within acceptable limits. This can be a time-consuming process and the details of these steps are often lacking in the currently available literature on the subject. For example, Jnitova et al. (2017) found that methodology rationale and model verification and validation was not always documented for the HR models presented in literature, while Uhrmacher et al. (2016) aimed to highlight the issue of a lack of reproducibility. It is the aim of this paper to begin to address both these issues in the process of verifying the FFM.

In order to verify the correctness of the FFM implementation, we will test that it behaves in a well-defined, predictable way as compared to a theoretical differential model (DM). The DM relates population changes to current population levels and flows. For piece-wise constant intake, exact solutions to the DM can be determined. Associated methods include the historically oft-used and well-understood Markov chain

method (Bartholomew et al. 1991) and related Linear Dynamical Systems which provide approximations to the exact solutions we consider here. The DM will be shown to be an effective benchmark against which to measure the aggregate behavior of the FFM (verification) as well as provide a useful diagnostic tool for the internal dynamics of this DES model (verification and validation).

The paper will begin with a high-level overview of the methodology we have developed for verification of the FFM in Section 2. This is followed by a description of the FFM for a military occupation in Section 3 including schemes for intake, internal transfer dynamics (i.e., promotions), and attrition. We chose a 4-rank model for simplicity in discussing and presenting results. Next, Section 4 will explain the FFM parameterization and mathematics of the DM for the exactly solvable scenario. Verification procedure of the FFM will then follow in Section 5 as we compare the aggregate results between the two methodologies for this carefully constructed scenario. The diagnostic power of the DM will then be examined with a closer look at the internal dynamics of the two modeling approaches in Section 6. A brief discussion of results and the way forward will conclude the paper.

2 VERIFICATION METHODOLOGY

In our model verification process, we will start with the development of an objective analytical tool, the DM, against which we can compare FFM results to verify that it performs exactly correct under set conditions in a regime where the differences between the internal dynamics of each model do not interfere. We will show that application of the DM is generalizable at the aggregate population level for all simulation times, as well as at sub-population levels during steady state only. In order to accomplish this, we will assert certain conditions in order to make the model comparison tractable.

As will be explained in more detail in the next section, individuals in the FFM leave the system by drawing a release date from a survival distribution every time they transfer between sub-populations (ranks). In order to remove the effects of these internal movements on the total population, we will take advantage of the memoryless property of an exponential survival distribution for a population. The memoryless property allows the survival time of any remaining individuals to be redrawn arbitrarily, without affecting the global population survival characteristics. This follows immediately: if a process is memoryless then one effectively does not know when a survival time was assigned, and so it does not matter if reassignment occurs for any surviving member. We use this invariance to resampling to match a simulated scenario to an exactly solvable analytical model, thereby making a strong verification test. While we will explore the details below, in brief the invariance to resampling ensures that flows between sub-populations (ranks in our case) do not affect aggregate level population dynamics. The implications are somewhat subtle, so we emphasize that this choice means that the mechanisms determining internal flows have no bearing at the aggregate level. This allows a differential population model to accurately describe the simulation, even if the internal flow mechanisms differ, albeit at the aggregate level. The differential population model, with its simple internal flow mechanism, can be solved exactly and we thereby obtain a very stringent verification test case.

In addition to verifying the aggregate population dynamics for our simulation's chosen internal flow mechanism, for our specific purposes we can verify the steady state population levels for each sub-population (rank). Given the parameters of the DM (attrition rates, promotion rates, and intake), the steady state populations can be determined. While this check is less general than the aggregate level verification we propose, discussion helps give context on how to approach both verification and validation and how the aggregate level verification results can be extended to a broader approach to quality assurance.

In short, by imposing a memoryless (exponential) distribution for survival times we can verify the population dynamics at arbitrary times at the aggregate level. As well, given suitable internal flow mechanisms, the steady state population for each sub-population can also be verified. In the following two sections we provide methodological details before presenting results.

3 FORCE FLOW MODEL (FFM) FOR A 4-RANK MILITARY OCCUPATION

The FFM is designed to capture the events of an individual's movement throughout their military career and to study their influence on the dynamics of a population. The model's architecture is purposely generic in the context of a military occupation in order to allow the flexibility to apply it to varying situations at any scale reasonable for the computing power available. Most scenarios under study are complex (hence the interest in modeling them) and we describe the architecture allowing this here, as well as how to specifically construct scenarios that can be solved analytically.

The hierarchical nature of military occupations presents unique challenges for personnel flow modeling and occupation management. New recruits primarily enter via the entry (bottom) rank and, through a series of training activities and promotions, they will be propelled upwards during their career. In the lowest ranks, individuals are often "pushed" to subsequent ranks until the individual reaches the Operational Function Point (OFP) in their occupation. After OFP, vacancies created in the ranks by attrition and promotions are filled internally by promotable individuals being "pulled" from the ranks below. This linear progression is characteristic of most military careers and captures the essential dynamics of a military occupation.

For the purposes of this paper, a simple 4-rank pull-promotion linear career progression for a single military occupation (Figure 1) will be used to verify that the FFM behaves as expected. As mentioned above, the simplest case of a hierarchical military career flow is a linear model in which the only considerations are inflow (intake), outflow (attrition), and transitions (promotions) through the system. A more realistic system would incorporate intake at any level (e.g., component transfers from the Reserve Force) as well as barriers to promotion in the model, such as minimum experience times or specific training requirements. However, these considerations increase the complexity of the system beyond this paper's scope, which is the fundamental verification of the underlying structure of the FFM, but will be investigated in detail in future work. We focus here on how to verify the model's general design by choosing parameters that match scenarios for which there is an exact solution.

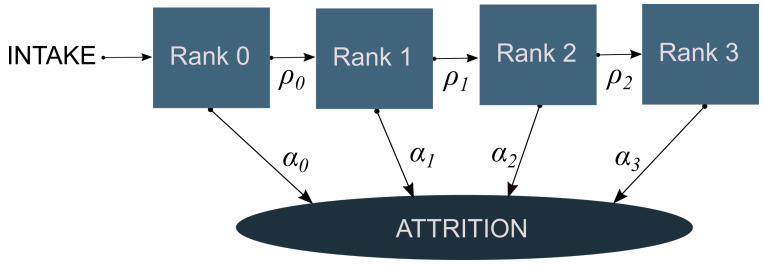

Figure 1: A simple 4-rank linear rank pull progression model for a military occupation. Flows out of ranks include rates of promotion (ρ_i) and attrition (α_i).

Following along with the career flow mapped in Figure 1, the logic contained within the FFM is described below. In military HR planning, transitions between ranks are often measured as annual promotion rates which we will denote as ρ while transitions out of the system are measured as annual attrition rates denoted as α.

3.1 Intake

For strategic planning purposes, military occupations within the CAF are assessed as a whole on an annual basis and as needed (Boileau 2012). As such, input parameters are imposed and output is measured at 1-year intervals. Simulated recruits are injected into the system through the entry rank (Rank 0 in Figure 1). The number of recruits that arrive annually is an input parameter to the FFM, with the entry date for each individual chosen at random from a uniform distribution over the course of the 1-year interval. For verification, entry occurs through the bottom rank only.

3.2 Promotions

In the CAF, the promotion policy is to allow a transition from a given rank to occur only if there is a vacancy in the established number of positions at the next rank. This is the primary policy that is most often modeled in a pull-promotion scenario.

In the FFM, this promotion policy is enforced by a simplified promotion rule which is applied on an individual basis for each promotion. In the CAF the established number of members in an occupation is determined through strategic assessment and is referred to as the Preferred Manning Level (PML). The following *Promote to PML* rule was used in the FFM: a vacancy created in a rank is instantly filled if someone promotable from the rank below is available. Vacancies will be filled via pull-promotions from the rank below until PML is reached or the "promotable list" is depleted. When a vacancy in a higher rank occurs, an individual is invited to move up from the promotable list. Promotions are drawn randomly from this list.

It should be noted that the *Promote to PML* rule is not necessarily one we would use when modeling a real occupation, but rather one that is deliberately chosen in order to match a suitable analytic model where steady state promotion rates are pre-determined (as described below in Section 4).

3.3 Attrition

In the FFM, attrition from the population is determined at the moment an individual enters a rank, be it via intake or promotion, by randomly drawing a release date from a survival distribution (described in further detail below). If the individual has not moved on via promotion by the time the attrition date arrives, then they are released and exit the system. Their release date is resampled upon every promotion to a higher rank via drawing from the appropriate survival distribution until they reach the top rank where they remain until their attrition date.

In order to match the FFM to an exactly solvable system, attrition in the FFM is modeled as a continuous memoryless process during verification. That is, the probability of an individual leaving does not depend on how much time they have spent in the system nor is it contingent on the amount of time that has passed since the last individual released. The only memoryless continuous probability distribution is the exponential distribution (Hoel et al. 1971) which has a probability density function given by

$$s(t) = \alpha e^{-\alpha t} \tag{1}$$

where α is the continuous time attrition rate. The expected survival time is then

$$\mathbb{E}[t] = \int_0^\infty t s(t) dt = 1/\alpha. \tag{2}$$

The FFM framework is constructed such that we can use any survival distribution, such as a simple uniform distribution or one built empirically from historical data. However, for verification purposes we use the exponential distribution for continuous attrition from an occupation parameterized using an annual attrition rate per rank (see Section 4). It is worth noting that for the sub-population of an individual rank i, as promotions increase so does the effective attrition out of that rank as $\alpha_i^{eff} = \alpha_i + \rho_i$.

The solid curve of Figure 2 shows an example of the probability to remain in a population that is undergoing continuous attrition at a rate of 10% ($\alpha = 0.1$). With no inflow, the population will decay at a timescale of 10 years according to Equation (2) for this setting of α. Considering a sub-population, the addition of a promotion rate increases the effective attrition rate, thus decreasing the effective survival probability. As an example, using the promotion rate for Rank 0 in our verification scenario ($\rho = 0.093$, see Section 6), the expected time to departing the rank nearly halves from 10 years to 5.18 years.

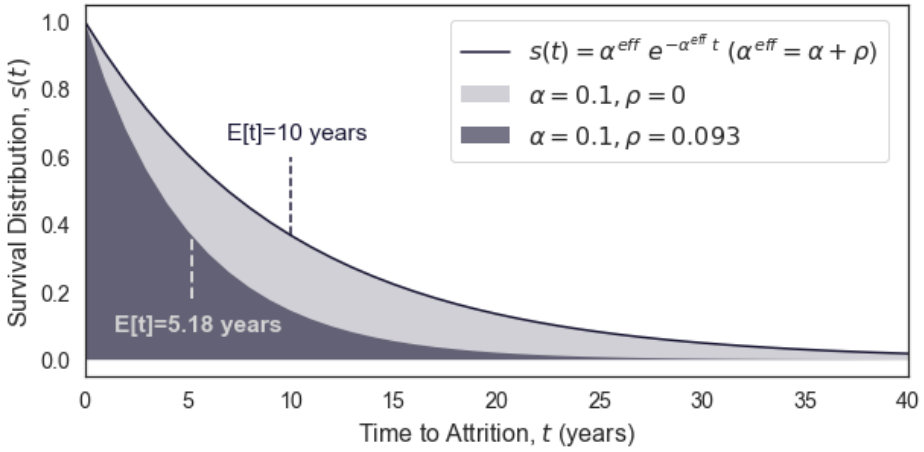

Figure 2: Exponential distribution for continuous attrition. The effective attrition for a rank sub-population includes the attrition rate plus the promotion rate ($\alpha^{eff} = \alpha + \rho$). The solid curve shows the probability to remain in the population for t years with attrition at an annual rate of 10%. The dark-shaded area shows the same probability with the addition of a promotion rate of 9.3% (see ρ_0 for Rank 0 for the verification scenario in Section 6).

4 A DIFFERENTIAL MODEL (DM) FOR RANK PROGRESSION

We would like to verify the FFM against a theoretical model and consider the evolution of both under specific circumstances to compare the results. To start, we will assume an exponential decay model with constant intake for the aggregate population P where the differential change in P over time t is given by

$$dP/dt = -\alpha P + r.$$

Note that this framework matches the exponential distribution used in the FFM. Here r represents a constant rate of inflow of people over time and outflow depends on the population P via the attrition rate α.

Additionally, we would like to capture the transitions between the ranks of Figure 1 where the intake to each rank is r for the entry rank and dictated by ρ for the subsequent ranks. We can generalize dP/dt as

$$d\mathbf{P}/dt = \mathbf{M} \cdot \mathbf{P} + \mathbf{R},$$

where $\mathbf{M}$ is a matrix that captures the transfers between sub-populations, $\mathbf{R}$ is the intake vector (for simplicity we use $\mathbf{R} = [r, 0, \cdots, 0]^T$), and $\mathbf{P}$ is now a vector describing sub-populations.

We can solve $d\mathbf{P}/dt$ exactly when $\mathbf{R}$ is constant (Higham 2008) and find the discrete time recurrence equation

$$\mathbf{P}(t+1) = \varphi_1(\mathbf{M}) \cdot [\mathbf{R} + \mathbf{M} \cdot \mathbf{P}(t)] + \mathbf{P}(t), \text{ with } \varphi_1(\mathbf{M}) = \frac{e^{\mathbf{M}} - \mathbf{I}}{\mathbf{M}} \tag{3}$$

where $e^{\mathbf{M}}$ is the "matrix exponential" and $\mathbf{I}$ is the identity matrix (Higham 2008). We consider 1-year time intervals which not only simplifies matters but is also a common convention in workforce planning. Equation (3) then becomes our Differential Model (DM). It is interesting to note that the DM can be related to an approximate discrete time Markov model, the standard approach taken in workforce modeling (Bartholomew et al. 1991), or associated Linear Dynamical System. However, unlike these approaches, there is no finite time step error in the DM.

To construct the matrix $\mathbf{M}$ we consider the flows into the given population P_i of rank i via the promotion rate from the rank below ρ_{i-1}. The outflows come from promotions out of the rank, ρ_i, and attrition α_i.

Recall that the constant inflow into the system **R** is not distributed among the ranks in this scenario but enters only via P_0. At the top, there are no promotions out, only attrition allows someone to exit the system (i.e., $\rho_3 = 0$).

The matrix **M** in Equation (3) for the n-rank generalized scenario of Figure 1 is then written as

$$\mathbf{M} = \begin{bmatrix} (-\alpha_0 - \rho_0) & 0 & \cdots & 0 \\ \rho_0 & (-\alpha_1 - \rho_1) & \cdots & \vdots \\ \vdots & \vdots & \ddots & 0 \\ 0 & \cdots & \rho_{n-1} & (-\alpha_n) \end{bmatrix}$$

Note that α from dP/dt has been substituted with $\alpha_i^{eff} = \alpha_i + \rho_i$. The diagonal determines the population that flows out of a rank over a time step and the off diagonal determines the population that is promoted into a rank.

We must now consider how best to set the parameters α_i and ρ_i. In particular, we would like to compare the aggregate behavior of the overall population P between the models as they evolve towards steady state. Using the DM developed above we can calculate exact steady state rates using Equation (3). We can substitute P_i for the target PML values, PML_i, and get

$$R^{SS} = \sum_{i=0}^{n} \alpha_i PML_i \text{ and } \rho_i^{SS} = \frac{\sum_{j=i+1}^{n} \alpha_j PML_j}{PML_i}. \tag{4}$$

We can readily see that R^{SS} will show us what we intuitively know must be true about the system: an intake value $R < R^{SS}$ will not allow P to reach PML, while an intake of $R > R^{SS}$ will exceed it.

We set the attrition rate equal for all ranks ($\alpha_i = \alpha$) which, combined with using a memoryless distribution, ensures internal flows do not modify attrition behavior, allowing aggregate analysis for verification purposes. As observed from the equation for the steady state promotion rates in Equation (4), α can be removed from the sum and the aggregate end state result will be reached irrespective of internal dynamics.

5 MODEL VERIFICATION: AGGREGATE DYNAMICS

We can now use the DM to verify aggregate level dynamics, in this case for the 4-rank linear progression described in the FFM of Figure 1. The FFM and the DM were compared using a growth-scenario involving a ten-fold increase in PML with trajectory towards steady state. This exaggerated parameter change was deliberately chosen to emphasize any differences between the FFM and the exact theoretical solution of the DM.

We set the attrition rate equal for all ranks ($\alpha = 0.1$). In the DM, promotion rates and intake are chosen such that PML will be reached at the steady state (i.e., R^{SS} and ρ^{SS}). All transitions between ranks are pull-type promotions in the FFM. The *Promote to PML* promotion rule will ensure the FFM and the DM will reach the same steady state, and the use of a memoryless distribution with equal attrition rates will ensure aggregate dynamics between the two models will match.

The FFM, like most DES models, is stochastic in nature allowing for variations in entry, promotion, and attrition times. The model was programmed in the ORIGAME environment (Okazawa 2013) and simulation outputs were averaged over 1000 replications. Flows in the FFM within each replication are whole number discrete events representing counts of individual movements within the system, as opposed to continuous real quantities allowed for in the DM. Results for the DM were generated by incrementally solving for $\mathbf{P}(t+1)$ of Equation (3).

Table 1 shows the input PML values for a hypothetical pyramidal rank structure. In both methods, the population was initiated at $P = 0$ and allowed to reach steady state PML values over a simulation time of 150 years. The PML for each rank, and consequently r, was then increased by an order of magnitude and

allowed to grow over another 200 year period. These simulation run periods were chosen to be long enough to ensure steady state results could be reliably measured. The fractional intake for the initial phase of the simulation was addressed in the FFM by randomly varying intake for each replication between $r = 19$ and $r = 20$ such that the mean over the 1000 replications gave $\bar{r} = 19.3$.

Table 1: FFM input parameters.

Simulation Time (years)	r	PML_0	PML_1	PML_2	PML_3	α_i
0 to 149	19.3	100	60	30	3	0.1
150 to 350	193	1000	600	300	30	0.1

Figure 3 (upper panel) shows the total population for the system from the time just before the growth period to 200 years afterwards. The dotted curves show the DM results from Equation (3) while the thicker step-function curve shows the sum of the steady state (SS) values set in Table 1 ($\sum_{i=0}^{3} PML_i = 1930$). The solid curve is the mean FFM result over 1000 replication of the DES while the lighter curves around them are a subset of the individual runs illustrating the variation between replications.

The overall growth of the total population in the FFM follows the DM by construction. The lower panel of Figure 3 shows the residual between the two models where the precision of the FFM replication results is expressed using the standard error of the mean (SEM) at time t over the $N = 1000$ replications. Visually, we can see that the mean FFM results are within one or two individuals from the DM, an acceptable fit for practical purposes. In order to quantify this closeness we chose to use the bounds given by Chebychev's inequality for its power as the strongest general statistical test (Hoel et al. 1971) that holds for non-Gaussian probability distributions, as is the case here. That is, we characterize the results as being statistically indistinguishable when the mean FFM result lies within kSEM from the analytical DM result $\geq(1-1/k^2)\%$ of the time (see Table 2). As the FFM results cover the DM results within the expected range we observe that they are statistically indistinguishable, a strong verification that the simulation is correctly constructed. The fact that the FFM results are generally slightly lower than the DM results is expected due to finite sample size effects, as the tail of the survival distribution (exponential of Figure 2) will be truncated under finite sampling and the expected value will be converged to from below.

We empirically measure the annual attrition rate from simulation results, calculated by dividing the number of individuals who left the system during a year a by the average population count over the same time period, or $\alpha(t) = a(t)/\frac{1}{2}(P(t)+P(t-1))$. Table 2 shows that during the simulation $\alpha \simeq 0.10008 \pm 0.00002$ with satisfying coverages over the set value of $\alpha = 0.1$.

Table 2: Mean aggregate results from the FFM and DM. Chebychev's inequality is used to compare the closeness of mean FFM results to DM results (minimum coverage of $(1-1/k^2)\%$ within $kSEM$).

			FFM	Coverage over DM		
Parameter		DM	Mean $\pm$ 1SEM	1SEM	$\sqrt{2}$SEM	2SEM
Population count	P	variable during growth phase		59%	76%	89%
	P^{SS}	1929.98	1929.21 $\pm$ 0.09	63%	82%	93%
Attrition rate	α	0.1	0.10008 $\pm$ 0.00002	63%	74%	90%
	α^{SS}	0.1	0.10006 $\pm$ 0.00002	59%	76%	89%

At this point we would like to highlight the importance of choosing the exponential as the survival distribution for the FFM (Equation 1) in order to verify it against the exact analytical solution of the DM. Figure 4 shows the same total population curves of the FFM and the DM in our verification scenario from Figure 3. The results of the simulation, with a uniform distribution in place of an exponential, are shown for comparison (red dashed curve). It is evident from Figure 4 that, while each survival scenario can be

parameterized to give the same aggregate steady state result, the path to steady state can vary significantly with only the exponential matching the DM along the entire simulation timeline. The uniform distribution was constructed by bounding it between 0 and a maximum of 20 years of service to give a mean $\mathbb{E}[t]$ of 10 years, matching the expected survival time of the exponential distribution with $\alpha = 0.1$ in Equation 2.

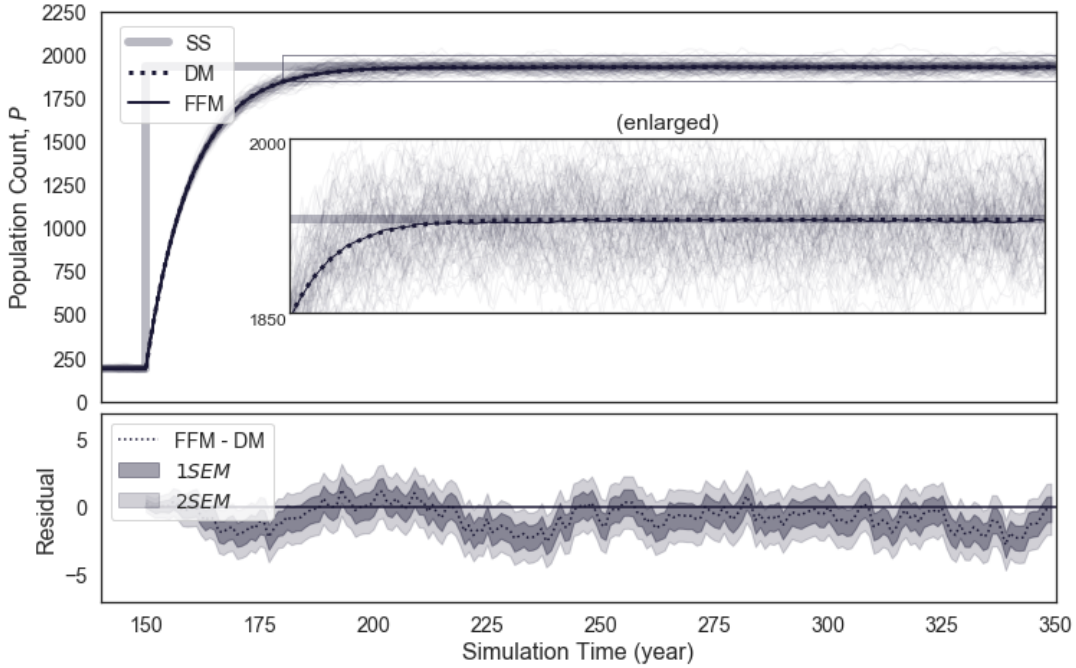

Figure 3: (*Upper panel*) Aggregate population count. Comparison of the DM and mean FFM results to the expected steady state (SS) value. A subset of the replications of the FFM are shown in the lighter curves around the mean result to demonstrate variability. (*Lower panel*) Residual between the FFM and the DM (dotted curve) with margins of standard error of the mean (SEM).

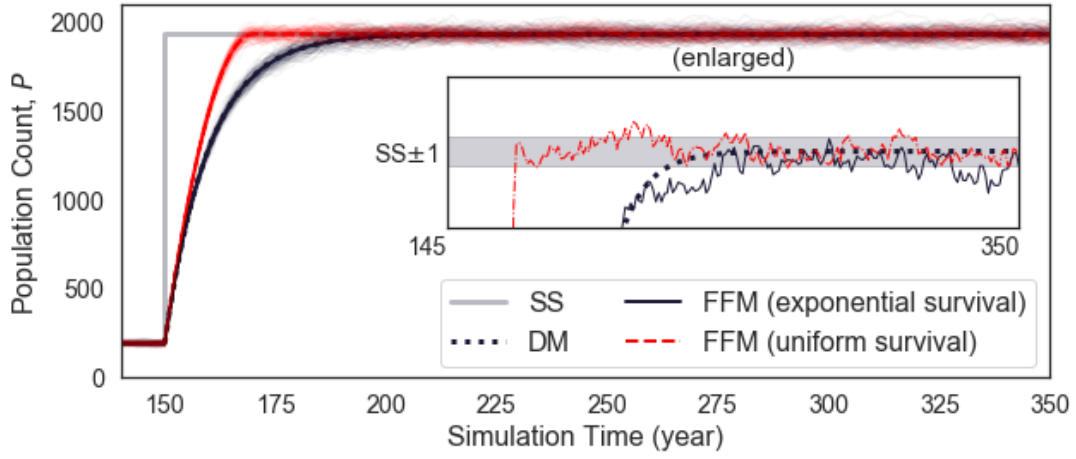

Figure 4: Survival distributions used in the FFM are contrasted by showing aggregate population results from the simulation using the exponential distribution of Equation 1 (black solid curve, see Figure 3) alongside results using a uniform distribution (red dashed curve).

6 MODEL DIAGNOSTICS: INTERNAL DYNAMICS

Setting the attrition rate equal for each rank allowed us to directly compare aggregate population totals between the FFM, the DM, and the expected steady state values since, by construction, the internal dynamics of the system do not affect those factors. Although P could be quite variable in the FFM between individual runs (Figure 3), its mean can be compared with the theoretical DM value and its error determined. However, while we carefully constructed our methodology to allow aggregate dynamics and steady state for rank populations to be analytically modeled, the internal flows are dictated by our promotion scheme which differs from the DM when the system is not in steady state. It is precisely in this regime outside of equilibrium where simulation demonstrates its utility. Examination of the system against the benchmark set by the DM is still useful as a diagnostic tool for the internal workings the FFM.

Figure 5 shows the population by rank for the FFM and DM. The steady state time threshold was chosen such that the difference between the FFM and steady state value reached a count of one individual, corresponding to a simulation year of 240 (see inset of the upper panel of Figure 5). By design, all ranks reach PML in steady state for both methods, though the internal path for each is observed to be quite different. As the steady state promotion rates are pre-calculated for the DM, progression at each Rank i follows a similar pattern of gradual rise to PML_i. The FFM, however, behaves quite differently due to the way in which internal transfers between the sub-populations (ranks) is governed. In the higher ranks (P_3 and P_2) where the population sizes are relatively small, the *Promote to PML* rule responds to the sudden ten-fold increase in PML by pulling promotions from below until PML_i is reached. Within a single year the upper two ranks have reached their target values. The lower two ranks (P_1 and P_0) are completely depleted during this rapid growth phase, dropping down to $P = 0$ before recovering. With the exception of the bottom rank (P_0), recovery is near instantaneous and P reaches PML faster than the DM rank populations. In the bottom rank, intake has been set such that $R = R^{SS}$ for the population to eventually recover and reach its steady state target value as evidenced in both Figures 3 and 5. There are no modeling artifacts that are preventing the population from reaching and maintaining the steady state target (SS). Note that the *Promote to PML* policy suppresses variation in the higher ranks.

Table 3: Mean internal results by rank for the steady state regime only. Chebychev's inequality is used to compare the closeness of mean FFM results to DM results (minimum coverage of $(1-1/k^2)\%$ within kSEM). Note that $\alpha_i^{eff} = \alpha_i + \rho_i$ where $\alpha_i = 0.1$.

			FFM	Coverage over DM		
Parameter		DM	Mean $\pm$ 1SEM	1SEM	$\sqrt{2}$SEM	2SEM
Population count	P_0	1000.00	999.21 $\pm$ 0.09	63%	80%	93%
	P_1	600.00	600 $\pm$ 0			
	P_2	300.00	300 $\pm$ 0			
	P_3	30.00	30 $\pm$ 0			
Intake Rate	R/P^{SS}	0.1	0.10007 $\pm$ 0.00005	39%	68%	85%
Effective Attrition rate	α_0^{eff}	0.193	0.1934 $\pm$ 0.0005	57%	72%	83%
	α_1^{eff}	0.155	0.1550 $\pm$ 0.0005	62%	81%	95%
	α_2^{eff}	0.11	0.1100 $\pm$ 0.0006	72%	90%	95%
	α_3^{eff}	0.1	0.100 $\pm$ 0.002	78%	90%	97%

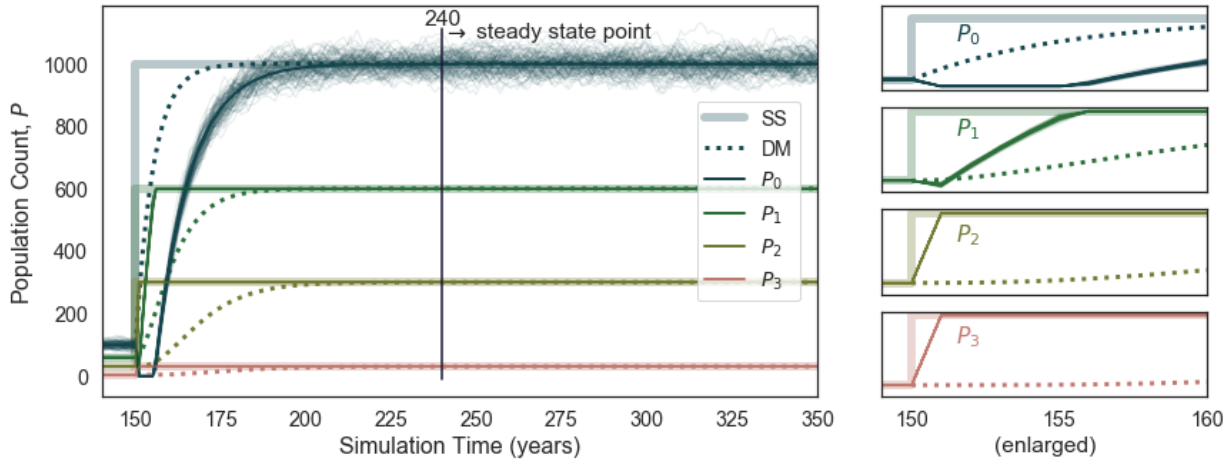

Figure 5: Population P_i counts by rank compared between the DM (dotted curves), the mean FFM results (solid curves), and the expected Steady State (SS) values (step function). A steady state point in time was chosen such that the difference between the FFM and steady state value reached a count of one individual, corresponding to a simulation year of 240. A subset of the FFM replications are shown in the lighter curves around the mean result to demonstrate variability.

We can further observe the difference between the FFM and the DM by examining the results of the promotion and attrition schemes used in the DES implementation during the growth phase. The left panel of Figure 6 shows the count of internal movements of the sub-populations via promotion as well as intake R. The right panel shows attrition counts from each rank.

Intake R is piecewise constant and immediately jumps from the initial value to ten-times more for the growth phase. Looking at the enlarged portions of the left panel of Figure 6, we can see from the immediate increase in promotions at every level above the steady state value during the first time interval of the growth period that the promotion rule *Promote to PML* has taken effect as soon as the ranks PMLs are increased ten-fold in the simulation. It is this internal logic of the FFM that causes $P_{1,2,3}$ to surpass their DM counterparts as seen in Figure 5. The initial spike in transfers out of P_1 and P_2 are sufficient to fill the upper ranks and the transfer levels rapidly even out to match steady state. Transfers out of the entry Rank 0 have a prolonged spike as it feeds the levels above it. Recall that there are no promotions out of the top rank ($\rho_3 = 0 \implies \alpha_3^{eff} = \alpha_3 = 0.1$).

Finally, we can check how our attrition scheme in the FFM performs against the expected attrition. Recall that as an individual progresses through their simulated career they draw a new attrition date from $s(t)$ (Equation (1)) upon entering a rank. By design, this resampling of the memoryless exponential distribution at every rank has no effect on the aggregate behavior shown in Figure 3. The right panel of Figure 6 compares the attrition counts a_i per rank. The pattern of attrition from each sub-population during the growth phase follows that of the corresponding rank population of Figure 5; when the population drops, so does the attrition count, as expected.

As vacancies draw transfers up through the ranks, the top level is filled first, then successively down through the chain. The R^{SS} is shown to be sufficient to drive the population of the FFM towards steady state as well as maintain equilibrium. Table 3 shows the mean effective attrition rates in the FFM simulation measured analogously to attrition rates $\alpha(t)$ for the aggregate population with coverage over the expected rates in steady state. Note the relatively high standard error at the highest rank. This is not wholly unexpected considering the small size of P_3 with a steady state of 30 individuals, consequently a single individual can have a significant relative impact on the total level compared to the target.

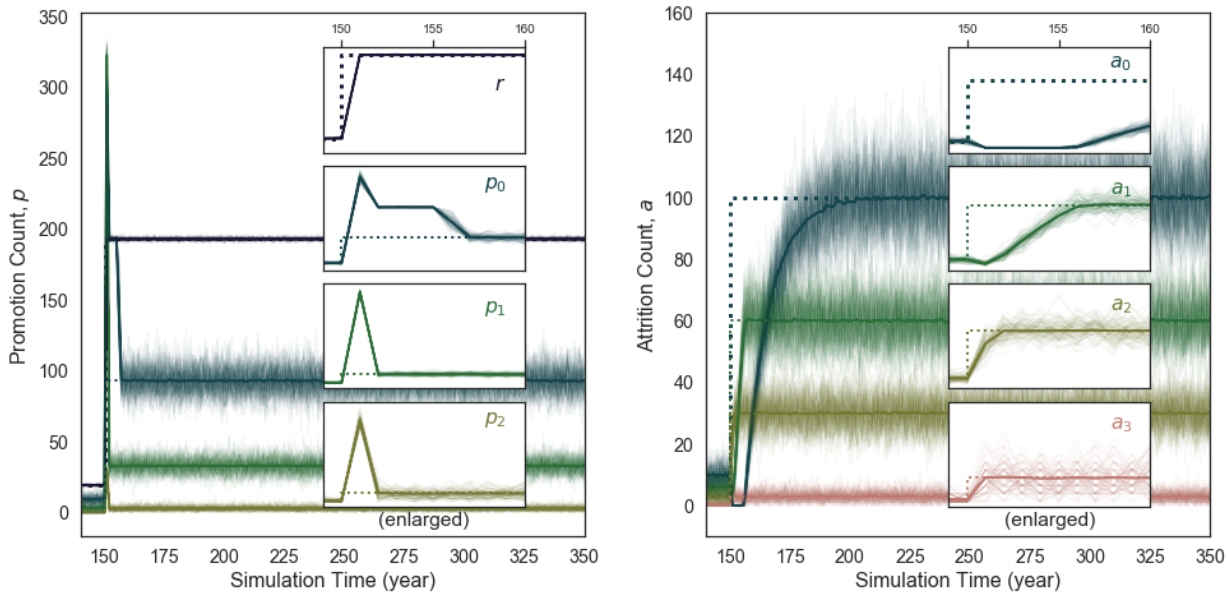

Figure 6: Promotion and attrition counts by rank, p_i (*left panel*) and a_i (*right panel*), compared between the mean FFM results (solid curves) and the steady state values set in the DM (dashed curves). Note that the intake r (recall $\mathbf{R} = [r, 0, \cdots, 0]^T$) is shown in the left panel along with promotion counts. A subset of the replications of the FFM are shown in the lighter curves around the mean result to demonstrate variability.

7 CONCLUSIONS

In this work we have aimed to take the discrete event workforce model of the FFM and map it to a regime where we can verify it analytically. We focused on how to verify a general architecture by selecting parameters that correspond to scenarios that we can exactly solve. As the goal was to verify aggregate behavior, we chose parameters in order to eliminate the aggregate level effects of internal dynamics. As a result, the verification methodology developed is agnostic to the internal workings of the model, such as the promotion policy. Using the exact solution to the analytical model, we were able to match the FFM to this scenario and compare output, confirming that the mean of the FFM is statistically indistinguishable from the theoretical solution to the DM.

The limitations of the verification methodology developed here include being confined to examine aggregate dynamics and sub-population steady state levels. However, the purpose of simulation is to accommodate more complex scenarios in the modeled systems and explore results generated under often unknown conditions. Thus, the method also proved useful outside of equilibrium as a benchmark against which we could critically examine the internal dynamics of the FFM, in particular the short-term effects of the attrition scheme and promotion policy on sub-population levels.

It is worth noting that the use of the exponential survival distribution in the FFM is necessary for its memoryless property, to construct a scenario against which the model's performance could be compared to an exactly solvable solution, and is commonly used in practice for military workforce planning models that use annual rates to predict attrition (Bartholomew et al. 1991). In real military populations, retention times also depend on contractual terms, age, and Years Of Service. While the investigation of a more realistic survival distribution built from historical data or estimated from policy is beyond the scope of this work, we acknowledge that this feature of the FFM, along with the inclusion of more realistic parameters, will alter the course of the simulation (indeed, this is why we simulate, Lucas et al. (2015)). This is expected and the DM offers a useful comparison to see how modeling choices alter simulated observations as we add complexity such as more realistic promotion rules and training to the model.

While the parameterization of the simulation required for verification may seem overly specialized, the simulation is exercised as a whole and its entire structure is therefore verified. In addition to the verification methodology presented here, other verification and validation efforts can supplement and extend checks. For example, examining results using "real world" parameterizations we are interested in, focusing on aspects not targeted by our verification (e.g., promotion policies), comparisons with historical data or other criteria, discussion of rules with subject matter experts, and other intuitive and widely-used approaches (Jnitova et al. 2017; Granberg and Nguyen 2018) will help ensure trustworthy results.

As the FFM is intended for use in decision making for the CAF, its verification is of particular importance. However, another goal of this work is to contribute a useful methodology to help ameliorate the present need for model verification and reproducibility in personnel management. The DM is shown to be a valuable addition to a quality assurance tool box alongside other validation approaches such as subject matter expert input and comparison against historical data. The strong verification case we present here, coupled with the aforementioned methods of validation, have increased confidence in the FFM for analysis of RCN occupations (Henderson and Arseneau 2018).

REFERENCES

Bartholomew, D., A. Forbes, and S. McClean. 1991. *Statistical techniques for manpower planning*. 2nd ed. Chichester, West Sussex, ENGLAND: Wiley.

Boileau, M. 2012. "Workforce Modelling Tools used by the Canadian Forces". In *Proceedings of The International Workshop on Applied Modelling & Simulation*, edited by A. Bruzzone, W. Buck, E. Cayirci, and F. Longo, WAMS2012, 18–23. Genoa, Italy: University of Genoa.

Granberg, T. A., and H. T. N. Nguyen. 2018. "Simulation based Prediction of the Near-Future Emergency Medical Services System State". In *Proceedings of the 2018 Winter Simulation Conference*, edited by M. Rabe, A. A. Juan, N. Mustafee, A. Skoogh, S. Jain, and B. Johansson, WSC '18, 2542–2553. Piscataway, NJ, USA: Institute of Electrical and Electronics Engineers, Inc.

Henderson, J., and L. Arseneau. 2018. "Modelling the Boatswain occupation from recruitment to release". Technical report, Defence Research and Development Canada, Ottawa, Canada. (DRDC-RDDC-2018-L369).

Higham, N. J. 2008. *Functions of Matrices: Theory and Computation*. Philadelphia, PA, USA: Society for Industrial and Applied Mathematics.

Hoel, P. G., S. C. Port, and C. J. Stone. 1971. *Introduction to probability theory*. Boston : Houghton Mifflin. Companion volume to the author's Introduction to statistical theory and Introduction to stochastic processes.

Jnitova, V., S. Elsawah, and M. Ryan. 2017. "Review of simulation models in military workforce planning and management context". *The Journal of Defense Modeling and Simulation* 14(4):447–463.

Lucas, T. W., W. D. Kelton, P. J. Sánchez, S. M. Sanchez, and B. L. Anderson. 2015. "Changing the paradigm: Simulation, now a method of first resort". *Naval Research Logistics (NRL)* 62(4):293–303.

Okazawa, S. 2013. "A Discrete Event Simulation Environment Tailored to the Needs of Military Human Resources Management". In *Proceedings of the 2013 Winter Simulation Conference*, edited by R. Pasupathy, S.-H. Kim, A. Tolk, R. Hill, and M. E. Kuhl, WSC '13, 2784–2795. Piscataway, NJ, USA: Institute of Electrical and Electronics Engineers, Inc.

Uhrmacher, A. M., S. Brailsford, J. Liu, M. Rabe, and A. Tolk. 2016. "Reproducible Research in Discrete Event Simulation: A Must or Rather a Maybe?". In *Proceedings of the 2016 Winter Simulation Conference*, edited by T. M. K. Roeder, P. I. Frazier, R. Szechtman, E. Zhou, T. Huschka, and S. E. Chick, WSC '16, 1301–1315. Piscataway, NJ, USA: Institute of Electrical and Electronics Engineers, Inc.

AUTHOR BIOGRAPHIES

JILLIAN ANNE HENDERSON is a defence scientist at the Department of National Defence. Dr. Henderson holds a PhD in Astronomy from the Universidad Nacional Autónoma de México. Her research interests lie in numerical modeling and simulation with a current focus on strategic military personnel management. Contact via email: Jillian.Henderson@forces.gc.ca.

ROBERT M. BRYCE is a defence scientist at the Department of National Defence. Holding a PhD in Physics from the University of Alberta, Dr. Bryce's research interests lie in explanatory data analysis–using theory, modeling, simulations, machine learning, graphing, and other tools. Contact via email: Robert.Bryce@forces.gc.ca.